Structure of the magnetic pileup boundary at Mars and Venus

C. Bertucci,[1,2] C. Mazelle,[1] M. H. Acuña,[3] C. T. Russell,[4] and J. A. Slavin[3]

Received 18 May 2004; revised 4 October 2004; accepted 2 November 2004; published 15 January 2005.

[1] The magnetic pileup boundary (MPB) is a sharp, thin, and well-defined plasma boundary located between the bow shock and the inner ionospheric boundary at comets, Mars, and Venus. This boundary separates the magnetosheath, a region of low magnetic fields with a conspicuous wave activity, from the magnetic pileup region dominated by strong, highly organized magnetic fields as a result of the pileup and draping of the interplanetary magnetic field. In the present paper we study the magnetic structure of the magnetic pileup boundary at Mars and Venus by means of the technique of minimum variance of the magnetic field. For each one of the crossings analyzed, we obtain a very well defined minimum variance vector. At Mars the direction of this vector agrees with the normal to the MPB fit obtained from Mars Global Surveyor crossings. The results confirm that the MPB is a well-defined plasma boundary. According to empirical criteria based on minimum variance analysis results, the Martian and Venusian MPB crossings would resemble an MHD tangential discontinuity rather than a rotational discontinuity. However, spacecraft observations suggest that the nature of the MPB could be far more complex. We compare our results with similar studies at the MPB of comets and the magnetic tail boundary of Titan, and we discuss the nature of the boundary from a general perspective.

Citation: Bertucci, C., C. Mazelle, M. H. Acuña, C. T. Russell, and J. A. Slavin (2005), Structure of the magnetic pileup boundary at Mars and Venus, *J. Geophys. Res.*, *110*, A01209, doi:10.1029/2004JA010592.

1. Introduction

[2] For many years the comparisons between the Martian and the Venusian solar wind interactions were limited mainly from the fact that the absence of a global dynamo-generated magnetic field at Mars had not been unambiguously demonstrated. In 1997 the observations by the Mars Global Surveyor (MGS) magnetometer (MAG) and electron reflectometer (ER) experiment [*Acuña et al.*, 1992] confirmed that the upper limit for a global dipole moment at Mars is $<\sim 2 \times 10^{17}$ A m^2. As a result, Mars does not possess a dynamo-generated, global-scale magnetic field, and the nature of its interaction with the solar wind is atmospheric, as for Venus and comets [*Acuña et al.*, 1998]. In addition, MGS MAG/ER revealed the presence of magnetic fields of crustal origin [*Connerney et al.*, 2001]. However, their influence is very limited both geographically (i.e., stronger in the Southern Hemisphere) and in altitude (upper limit of the ionosphere), and therefore they do not significantly influence the global solar wind interaction [*Acuña et al.*, 1998].

[3] During the aerobraking phase of the MGS mission, highly elliptical orbits provided an excellent coverage in altitude in order to characterize the different plasma regions and boundaries. First, the spacecraft identified a fast bow shock, where the solar wind plasma is strongly decelerated and heated. Second, MGS detected the magnetosheath, a very turbulent region with an important wave activity. Below the magnetosheath, MGS MAG/ER detected the magnetic pileup region (MPR). This region is dominated by strong, highly organized magnetic fields as a result of the pileup and draping of the interplanetary magnetic field lines over the highly conducting obstacle represented by the ionosphere. The magnetic pileup region extends into the nightside as the magnetic tail lobes.

[4] In opposition to gas dynamic descriptions, MGS MAG/ER data showed that the transition from the magnetosheath to the MPR was not gradual. These two regions were in fact unmistakably separated by a thin plasma boundary: the magnetic pileup boundary (MPB) [*Acuña et al.*, 1998]. This name was originally used to identify a similar boundary detected around comet P/Halley from Giotto spacecraft observations [*Neubauer*, 1987; *Mazelle et al.*, 1989]. Thus the MPB is at the same time the inner boundary of the magnetosheath and outer boundary of the MPR. MGS MAG/ER observations showed that the MPB also extends into the nightside and separates the tail lobes (or MPR) from the magnetosheath [*Nagy et al.*, 2004].

[5] At first, the Martian MPB was unambiguously identified by MGS MAG/ER by three simultaneous features: a usually strong jump in the magnetic field magnitude, a drop in the magnetic field fluctuations both in direction and magnitude, and a strong decrease in the superthermal electron fluxes. These signatures led *Vignes*

[1]Centre d'Etude Spatiale des Rayonnements, CNRS/UPS, Toulouse, France.
[2]Now at Blackett Laboratory, Imperial College London, London, UK.
[3]NASA Goddard Space Flight Center, Greenbelt, Maryland, USA.
[4]Institute of Geophysics and Planetary Physics, University of California, Los Angeles, California, USA.

Copyright 2005 by the American Geophysical Union.
0148-0227/05/2004JA010592$09.00

et al. [2000] to deduce the mean position and shape of the boundary by fitting a conic section to 488 crossings.

[6] The Martian MPB had been already crossed by previous missions [see, e.g., *Vaisberg*, 1992], but its nature remained a controversial subject for many years since the question of the existence of an intrinsic, global, dynamo-generated magnetic field had not been resolved [see, e.g., *Slavin and Holzer*, 1982; *Zakharov*, 1992; *Russell*, 1978a, 1978b]. The variety of names employed to designate this boundary (most of them used in works using Phobos 2 measurements) reveals the discrepancies in its interpretation. As an example, the term "magnetopause" was used to refer to this boundary, as a strong global-scale dynamo-generated magnetic field was believed to exist [*Lundin et al.*, 1990]. On the other hand, names such as "planetopause" [*Trotignon et al.*, 1996], "protonopause" [*Sauer et al.*, 1992], or "plasma composition boundary" [*Breus et al.*, 1991] were used to describe the strong changes in the predominant ion population that take place at this boundary.

[7] This controversy ended when *Vignes et al.* [2000] compared their MPB fit with the *Trotignon et al.* [1996] fit of the so-called planetopause from Phobos 2 spacecraft data (with a sparse coverage on the dayside) and showed that the planetopause (and therefore the so-called magnetopause, plasma composition boundary, and protonopause) and the MPB are the same plasma boundary. This important conclusion led to a reinterpretation of some of the Phobos 2 observations and then to a more complete description of the boundary. Thus Phobos 2 measurements provided essential information on the changes in the plasma properties at the MPB: an increase in the total electron density [*Grard et al.*, 1989], as well as a decrease in the density and the axial velocity of solar wind ions, as planetary ions begin to dominate [*Lundin et al.*, 1990; *Sauer et al.*, 1992]. A complete discussion on the Martian MPB based on MGS and Phobos 2 measurements is given by *Nagy et al.* [2004].

[8] Further analysis of MGS data provided new signatures to identify the Martian MPB. *Bertucci et al.* [2003a] have recently reported, using MGS MAG data, that the draping of the interplanetary magnetic field lines is dramatically enhanced at the MPB. Unexpectedly, the same enhancement has been reported recently at Venus, where the MPB had never been reported. Using Pioneer Venus Orbiter (PVO) magnetometer (OMAG) measurements, *Bertucci et al.* [2003b] show that a dramatic change in the magnetic field topology takes place across a very thin layer or boundary on the dayside of Venus, at altitudes well above the ionopause and compatible with the external boundary of the magnetic barrier as defined by *Zhang et al.* [1991] from magnetic pressure values. This particular change in the magnetic field structure allowed *Bertucci et al.* [2003b] to identify for the first time on the dayside of Venus a boundary with the same properties as the cometary and Martian MPB.

[9] Figure 1 compares the magnetic field observations around Mars and Venus by MGS and PVO, respectively. Figure 1a shows MGS MAG data for a near-terminator orbit, between 150 and 5500 km altitude ($\sim$1.04 to $\sim$2.62 R_M aerocentric distance; 1 R_M = 1 Martian radius = 3380 km). The magnetic field is expressed in spherical Mars-centered solar orbital coordinates (MSO). The elevation over the ecliptic θ, the azimuth φ (0° = sunward), and the magnetic field magnitude are depicted in the upper three panels, whereas the fourth panel shows the spacecraft altitude. The bow shock (BS) is crossed around 0734 UTC. A few minutes before, the spacecraft is in the magnetosheath, a region characterized by a conspicuous wave activity. The MPB appears as a very sharp discontinuity (vertical dashed lines) crossed around 0702 UTC at 1180 km altitude ($\sim$1.35 R_M distance) at $\sim$83° solar zenith angle (SZA) and at $\sim$0800 local time (LT). This boundary distinctly separates the magnetosheath from the MPR or magnetic barrier region. The magnetic field and the plasma undergo drastic changes at the MPB. $|B|$ goes from 10 up to 25–30 nT in <1 min, whereas the fluctuations in the magnetic field orientation abruptly decrease. The MPR is characterized by smoothly varying, piled-up fields that form the magnetic barrier on the dayside. In this case, $|B|$ in the barrier peaks at $\sim$43 nT, whereas near the periapsis, the magnetic field decreases sharply, as MGS enters the ionosphere.

[10] Figure 1b displays the magnetic field between 360 and 6460 km altitude ($\sim$1.06 and $\sim$2.07 R_V distance; 1 R_V = 1 Venusian radius = 6050 km) in spherical Venusian solar orbital (VSO) coordinates. The VSO coordinate system is defined in a similar way as the MSO. Inside the bow shock the magnetic field in the magnetosheath also displays large-amplitude wave activity both in direction and magnitude. As in Figure 1a, the MPB (vertical dashed lines) clearly separates the magnetosheath and the magnetic pileup region. The boundary is easily identifiable at $\sim$660 km altitude ($\sim$1.11 R_V distance) by a sharp jump in $|B|$ (a factor of 2.5) followed by a decay in the magnetic field fluctuations, particularly obvious in the magnetic field orientation. In the MPR the magnetic field magnitude reaches 87 nT. The ionospheric boundary in both cases is located on the right, below the MPR.

[11] The recent results about the Martian and the Venusian MPB thus demanded a more detailed description of the magnetic structure of these two boundaries. The data to be used in such a study must have a time resolution high enough to have several samples within the boundary. At Mars and Venus the MPB is only a few hundred kilometers thick, so only the magnetic field data assure a reasonable number of measurements within the boundary.

[12] In this work we analyze the magnetic structure of the Martian and Venusian MPB by using minimum variance analysis (MVA) on magnetometer data for several boundary crossings by MGS and PVO. We search for the vector normal to the local current sheet and, for each crossing of the Martian MPB, we compare the normal vector obtained from MVA with the normal vector expected for a MPB fit from 1149 MGS crossings using the same technique as *Vignes et al.* [2000]. Finally, we study the normal and tangential magnetic field components to characterize the nature of the discontinuity.

2. Method and Results

[13] The MVA for a single spacecraft introduced by *Sonnerup and Cahill* [1967] and extensively treated in

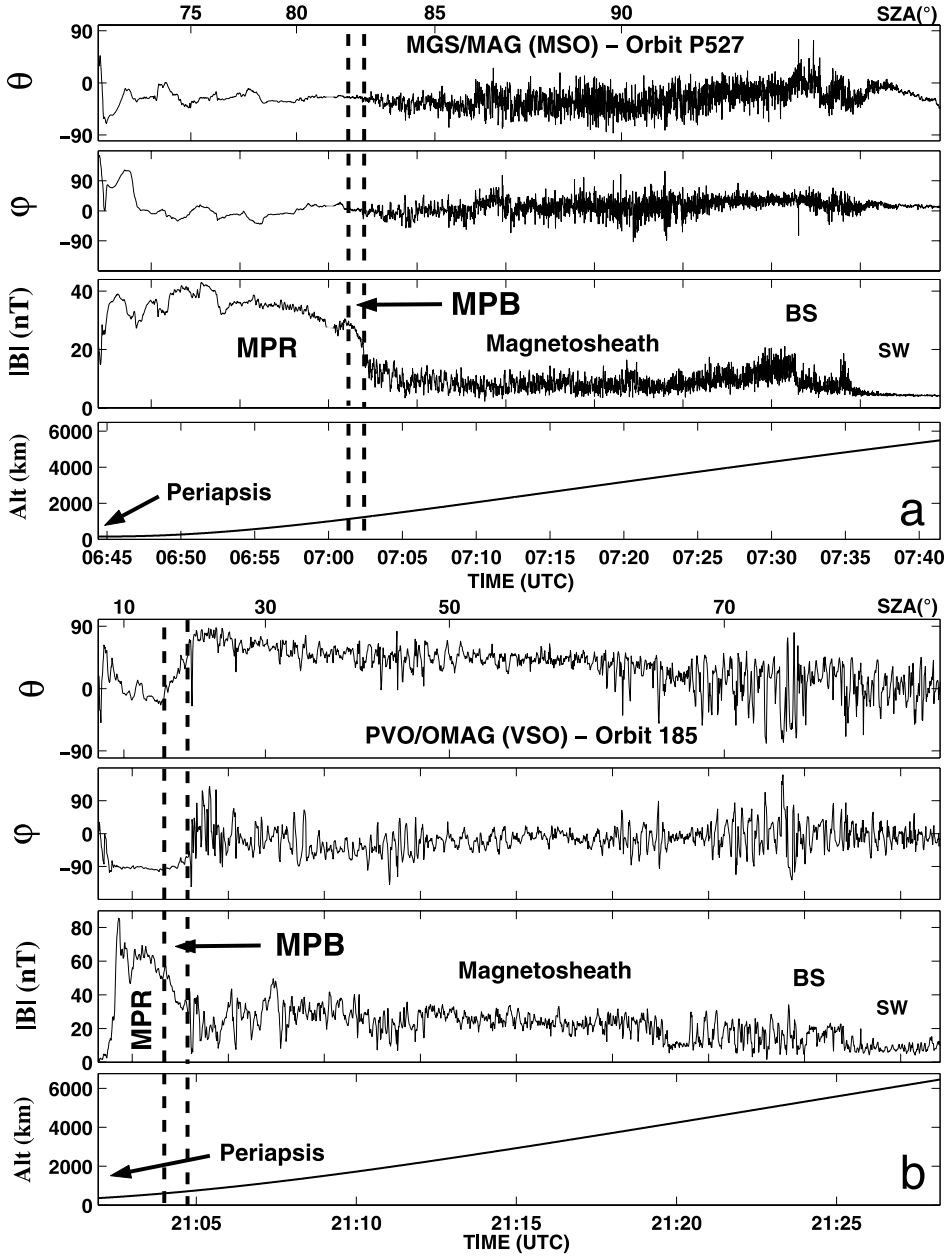

Figure 1. Comparison between the magnetic field measurements at Mars and Venus. (a) MGS MAG data in spherical Mars-centered solar orbital (MSO) coordinates for a near-terminator orbit, between 150 and 5500 km altitude. MPB is crossed around 0702 UTC at 1180 km altitude at ~83° solar zenith angle (SZA) and at ~0800 LT. (b) Pioneer Venus Orbiter (PVO) magnetometer (OMAG) data in spherical Venusian solar orbital (VSO) coordinates, between 360 and 6460 km altitude. MPB is crossed at ~660 km altitude and ~18° SZA [after *Bertucci et al.*, 2003b].

recent works [e.g., *Sonnerup and Scheible*, 1998] has been successfully used in the study of plasma boundaries such as the Earth magnetopause or the magnetic tail boundary of atmospheric, weakly magnetized bodies [e.g., *Slavin et al.*, 1986; *Saunders and Russell*, 1986]. It is well known that if the structure of a plasma boundary is one dimensional, the variations along the boundary occur on length scales much greater than its thickness, and the magnetic field component normal to the boundary must remain constant. The MVA is used as an approximation to obtain the normal vector by determining the minimum variance direction. This direction is given by the normalized vector $\mathbf{e}_3$ associated to the smallest eigenvalue λ_3 of the covariance matrix M_{ij}:

$$M_{ij} = \langle B_i B_j \rangle - \langle B_i \rangle \langle B_j \rangle, \tag{1}$$

where $i, j = x, y, z$, and the average is calculated for the interval of analysis. The normal vector $\mathbf{n}$ is then parallel to $\mathbf{e}_3$ and points outside the boundary. On the other hand, the

eigenvectors $\mathbf{e}_1$, $\mathbf{e}_2$, corresponding to maximum (λ_1) and intermediate (λ_2) variances, respectively, form with $\mathbf{e}_3$ an orthonormal set of vectors. This permits obtaining the normal component of the average magnetic field ($\mathbf{B}_0$) in the interval: B_n.

[14] In the present work the errors in the orientations of the eigenvectors and in the components of the average magnetic field in the eigenvector base are supposed to be only statistical (neither systematic errors nor nonstationarity effects are considered). Therefore these errors will only depend on λ_1, λ_2, and λ_3, as well as on the number of vectors N.

2.1. MGS Observations at Mars

[15] Figure 2 (left) shows MGS MAG data in the surroundings of the MPB crossing for orbit P342 (1348:23–1349:06 UTC), unambiguously identified from the signatures on MGS MAG/ER data described in section 1. Once the thin layer representing the MPB was established by these independent criteria, we applied MVA within it to be sure that the current sheet is associated to the boundary itself and not related to other structures as high-amplitude low-frequency waves. For this crossing, MVA was applied from 1348:18 to 1348:38 UTC (the interval is indicated with two dashed lines). The resulting intermediate-to-minimum eigenvalue ratio is $\lambda_2/\lambda_3 = 26.9$ (whereas $\lambda_1/\lambda_2 = 6.1$) for $N = 634$ vectors, indicating that the minimum variance vector is well defined. Furthermore, the mean magnetic field component along the boundary normal ($B_n = 2.5 \pm 0.2$ nT) is quite small compared with the mean field magnitude ($|B_n|/B_0 = 0.12$), revealing that the mean magnetic field is nearly tangential. As a result the magnetic field lies mainly in the ($\mathbf{e_1}$, $\mathbf{e_2}$) plane, where it describes a counterclockwise rotation. The errors in the eigenvector directions and in B_n were calculated from equations by *Sonnerup and Scheible* [1998, equations 8.23 and 8.24]. In Figure 2 (right), two hodograms describe the magnetic field components along the maximum and intermediate variance directions (B_1 and B_2) and the maximum and minimum variance directions (B_1 and B_3) between 1348:28 and 1348:33 UTC.

[16] We then compared the value for the angle Ψ between the minimum variance vector and the vector normal to the ellipsoid representing the mean location of the MPB from 1149 MGS crossings based on *Vignes et al.* [2000] work. The normal vector is taken at the intersection between the surface and the spacecraft mean position vector for the analyzed interval. In the case shown in Figure 2, $\Psi = 12° \pm 0.2°$.

[17] Once the normal vector has been obtained, we can estimate the thickness of the boundary h assuming that its position does not vary during the crossing (to avoid this assumption we should need four spacecraft in the more general case). In general, we expect that the smaller the angle between the normal and the spacecraft average velocity vector during the crossing (supposing that the spacecraft trajectory within the boundary layer can be approximated by a straight line), the smaller the time of crossing.

[18] However, it is likely that the MPB thickness varies with SZA precluding the possibility of calculating h accurately. Still, $h' = |(\mathbf{r}_{\text{entrance}} - \mathbf{r}_{\text{exit}}) \cdot \mathbf{n}|$ (where $\mathbf{r}_{\text{entrance}}$ and $\mathbf{r}_{\text{exit}}$ are the spacecraft position at the apparent entrance/exit to and from the MPB) remains a very good approximation to h for single-spacecraft observations. When ($\mathbf{r}_{\text{entrance}} - \mathbf{r}_{\text{exit}}$) and $\mathbf{n}$ are parallel, $h' = h$. In this case, $h' = 80$ km for SZA $\sim 63°$. The distance between the spacecraft mean position within the boundary and the ellipsoid is $\delta = 0.073\ R_M \cong 248$ km.

[19] If we suppose that the MPB is a stationary plane surface of infinitesimal thickness (h is negligible with respect to the MPB curvature radius), the current density along the boundary can be estimated from the continuity condition derived from the Maxwell-Ampère equation across a discontinuity. Indeed, if $\mathbf{n}$ is the normal vector to that surface and if $\mathbf{B}_u$ and $\mathbf{B}_d$ are the magnetic field vectors measured upstream and downstream from the boundary, the surface current density $\mathbf{J}_S$ along the boundary is given by

$$\mathbf{J}_S = (1/\mu_0)[\mathbf{n} \times (\mathbf{B}_u - \mathbf{B}_d)]. \quad (2)$$

[20] The volume current density $\mathbf{J}_V$ along the MPB can be calculated by dividing $\mathbf{J}_S$ by the boundary thickness h provided that $\mathbf{J}_S$ does not vary along the MPB normal. $\mathbf{B}_u$ and $\mathbf{B}_d$ were calculated by averaging the magnetic field within intervals upstream and downstream from the boundary, respectively. These intervals were chosen as to be outside but contiguous to the MPB as defined from MAG/ER data. As a result the surface current density is 6.5×10^6 nA m^{-1}. If we invoke the assumptions made for the estimation of the MPB thickness, we can use $h' = h$, and then the volume current density flowing along the MPB gives in this case $|\mathbf{J}_V| = 81$ nA m^{-2}. Recent three-dimensional bi-ion bifluid simulations [*Harnett and Winglee*, 2003b] predict volume current density values between 30 and 40 nA m^{-2} at the magnetic pileup boundary location (E. M. Harnett, private communication, 2004). These values are therefore similar if one considers that the empirical estimation is made from single-spacecraft observations. Moreover, these simulations underestimate the contribution of certain terms of Ohm's law, which leads to an underestimation of the volume current density. As a result the values given by these models would represent up to 30% of the real value (E. M. Harnett, private communication, 2004), which is consistent with our results.

[21] Table 1 illustrates the results of the MVA analysis for several MGS MPB crossings between 35° and 91° solar zenith angle (SZA), including the intermediate-to-minimum eigenvalue ratio (λ_2/λ_3), the number of points (N), B_n, θ_{Bn} (the angle between $\mathbf{n}$ and $\mathbf{B}_0$), the ratio between $|B_n|$ and $|B_0|$, the angle Ψ, and δ. The λ_2/λ_3 values are >7.0, while $76.8° \leq \theta_{\text{Bn}} \leq 103.5°$, showing that $\mathbf{B}_0$ is tangential. It is interesting to note the good agreement between MVA and fit normal vectors ($\psi < 13.9°$). Figure 3 illustrates this by comparing the minimum variance direction and the normal vector to the MPB fit for the crossings listed in Table 1.

2.2. PVO Observations at Venus

[22] The same analysis was performed on OMAG data across the Venusian equivalent of the MPB, identified on the dayside according to the following criteria: enhancement of the magnetic field draping [*Bertucci et al.*, 2003b] and/or presence of a sharp gradient in the magnetic field magnitude

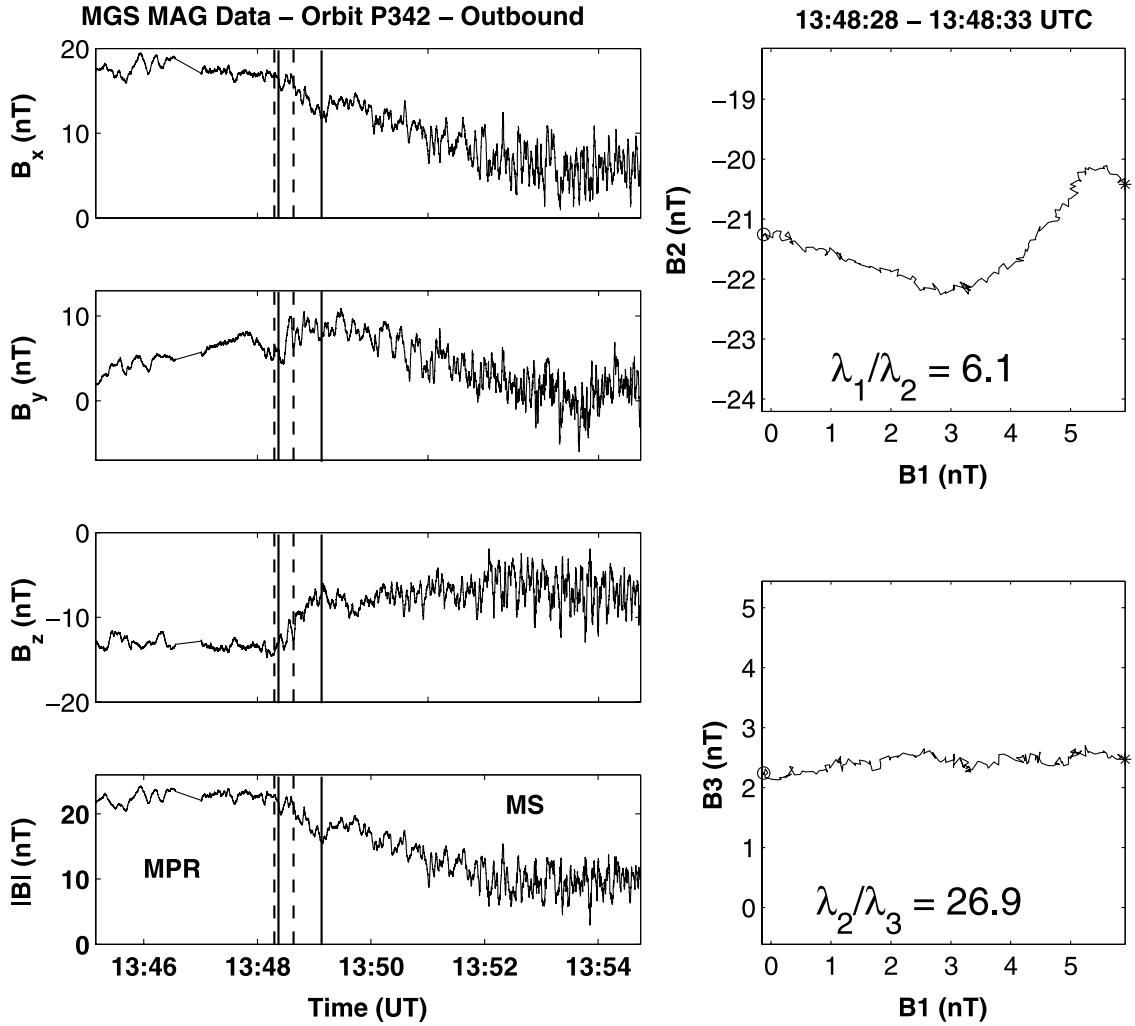

Figure 2. High-resolution (32 s^{-1}) MGS MAG data (MSO coordinates) for a Martian MPB crossing (solid lines) on orbit P342 around 63° SZA. MVA is applied between 1348:18 and 1348:38 UTC (dashed lines). Magnetosheath (MS) and the magnetic pileup region (MPR) are indicated for reference. On the right, two hodograms show the magnetic field projection on the minimum variance planes ($\mathbf{e_1}$, $\mathbf{e_2}$) and ($\mathbf{e_1}$, $\mathbf{e_3}$) between 1348:28 and 1348:33 UTC. Start and the end of the hodograms are marked with circles and stars, respectively. Eigenvalue ratios are also indicated.

followed by a decrease in the fluctuations in the magnetic field direction and magnitude. Figure 4 shows the results for orbit 185. The left panels show the magnetic field in VSO coordinates. The interval of analysis (2103:57–2104:18 UTC) is marked again with two dashed lines. Two panels on the right of Figure 4 show hodograms of the magnetic field vector in that interval. The eigenvalue ratios $\lambda_2/\lambda_3 = 12.0$ and $\lambda_1/\lambda_2 = 4.3$ for $N = 114$ show that the normal vector is well determined. The magnetic field component in that direction is $B_n = -14.9 \pm 1.2$ nT, but its value relative to the magnitude of mean magnetic field is not as small as for the Martian case shown earlier ($|B_n|/|B_0| = 0.32$). Table 2 illustrates the results of the minimum variance analysis for several Venusian MPB crossings, covering the subsolar region (SZA $\leq$ 56°). The angle 92.3° < θ_{Bn} < 110.1°, which for these few examples does not seem to correlate with

Table 1. Main Parameters of the MVA for Different Martian MPB Crossings by MGS and Comparison With the Normal to the Ellipsoid Representing the Average MPB Position Calculated From 1149 Crossings

Orbit	SZA, deg.	Altitude, km	λ_2/λ_3	N	B_n, nT	θ_{Bn}, deg.	$\lvert B_n\rvert/\lvert B_0\rvert$	Ψ, deg.	δ, R_M
P33	64	2044	8.9	148	5.1 ± 0.6	78.6 ± 1.8	0.20	3.3 ± 1.4	0.339
P226	35	1259	9.4	59	−3.1 ± 1.0	97.9 ± 2.8	0.14	12.7 ± 1.4	0.145
P342	63	1118	26.9	634	2.5 ± 0.2	83.3 ± 0.5	0.12	12.0 ± 0.2	0.073
P486	91	1146	10.6	223	0.7 ± 0.2	87.7 ± 1.3	0.04	9.8 ± 1.0	0.123
P527	82	1227	18.4	554	1.7 ± 0.2	85.4 ± 0.6	0.08	3.4 ± 0.6	0.026
P1180	44	572	7.0	240	−5.7 ± 0.5	101.9 ± 1.6	0.21	12.0 ± 0.8	0.055

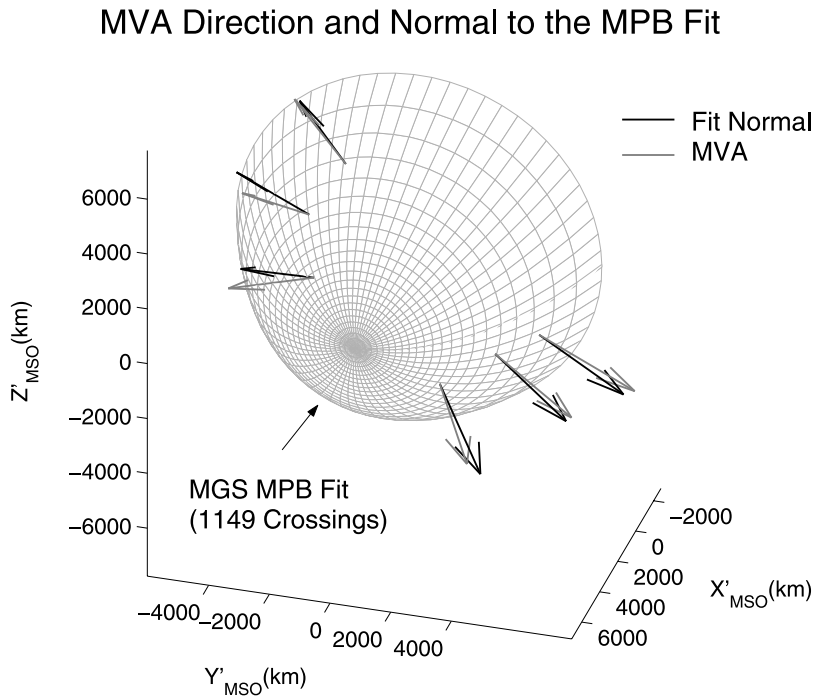

Figure 3. Comparison between minimum variance direction and the normal expected from a MPB ellipsoid fit from 1149 Martian MGS crossings based on *Vignes et al.* [2000] work (blue arrows). Sketch is represented in 4°-aberrated MSO coordinates. See color version of this figure at back of this issue.

SZA. This shows that as for the case of Mars, $\mathbf{B}_0$ is nearly perpendicular to the boundary normal. The absence of a fit representing the average position of the Venusian MPB precludes a comparison similar to that made for Mars.

3. Discussion and Conclusions

[23] The results presented in this study clearly show that the Martian and Venusian MPB have a distinct local normal vector revealing the presence of a well-defined current sheet on the maximum and intermediate variance plane. The average magnetic field is in general nearly perpendicular to the normal vector regardless of the solar zenith angle. Furthermore, the results show that the normal vector deduced from MVA is in general compatible with the direction of the normal to the surface representing the mean position and shape of the MPB, at least in the case of Mars. This confirms the consistency between the model proposed by *Vignes et al.* [2000] and the local structure of the boundary. At the same time the magnetic field lines, which are tangential to the MPB surface according to our results, "follow" the shape of the MPB in a clear draped configuration. This is in agreement with the dramatic enhancement of the magnetic field line draping reported at the MPB [*Bertucci et al.*, 2003a, 2003b].

[24] For some of the MPB crossings the direction of the normal vector, though very well determined, is not compatible with the normal to the MPB fit. These crossings usually occur near the terminator and very close to the fit, suggesting that the MPB could have a corrugated shape. However, only a study on a larger number of orbits could give clues on the spatial distribution of these undulations. The crossing furthest away from the mean MPB position occurs during orbit P33 ($\delta \cong 1150$ km). Interestingly, Ψ is small, leading to the idea that the boundary may also experience expansions and compressions. This is consistent with the fact that the dispersion in the positions of the MPB crossings by MGS increases with increasing SZA [*Vignes et al.*, 2000]. Asymmetries in the position of the Martian MPB may also contribute to discrepancies between the normal vectors obtained from MVA and from the MPB fit. Several models suggest that the MPB position may be influenced by the presence of crustal magnetic fields [*Harnett and Winglee*, 2003a] and by the direction of the motional electric field [*Brecht*, 1997]. *Crider et al.* [2002] report a weak dependence of the MPB position upon crustal fields.

[25] On the other hand, the normal to the Martian MPB could be a good approximation to the normal to a putative pressure balance boundary (i.e., "ionopause") separating the MPR and the ionosphere, as long as certain conditions are satisfied. First, the thermal pressure in the ionosphere must be high enough to counterbalance the solar wind dynamic pressure; second, the MPB must be as close as possible from the ionosphere (the MPB is further from the ionosphere with increasing SZA); and third, the influence of magnetic crustal fields must be negligible. The vertical component of the magnetic field is important in the Southern Hemisphere at altitudes below 400 km [*Connerney et al.*, 2001]. This is interpreted as possible minicusps of crustal fields that affect the height of the ionosphere [*Mitchell et al.*, 2001]. All these factors reduce the region where this agreement could be expected almost to the subsolar region.

[26] Although the assumption of one dimensionality is difficult to substantiate due to the use of single spacecraft

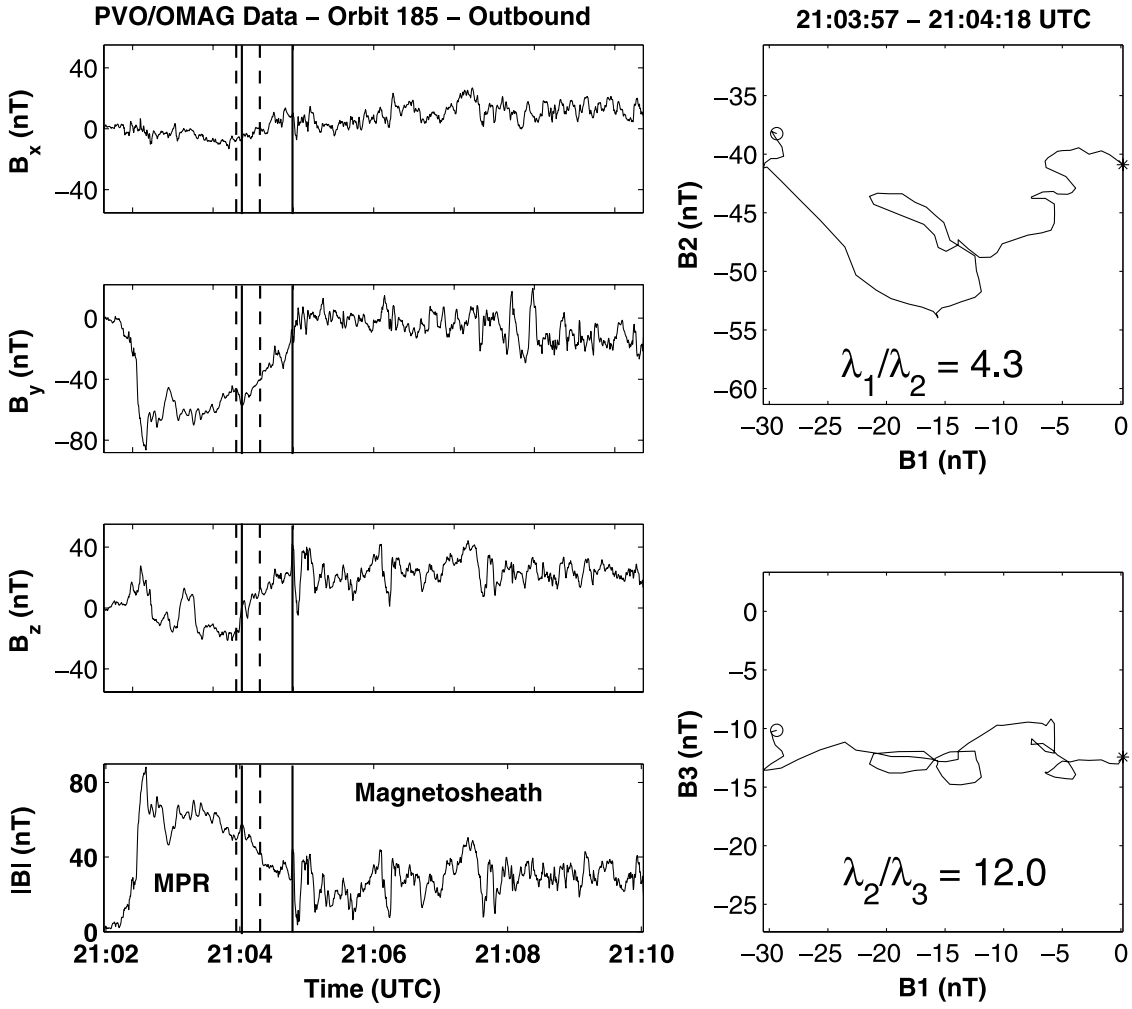

Figure 4. High-resolution (4 s^{-1}) PVO/OMAG data (VSO coordinates) around a Venusian MPB crossing (solid lines) on orbit 185 around 17° SZA. MVA is applied between 2103:57 and 2104:18 UTC (dashed lines). On the right, hodograms show the magnetic field components on the minimum variance planes ($\mathbf{e_1}$, $\mathbf{e_2}$) and ($\mathbf{e_1}$, $\mathbf{e_3}$). Start and the end of the hodograms are marked with circles and stars, respectively. Eigenvalue ratios are also indicated.

and the absence of ion measurements, the superthermal electron measurements by MGS ER have been useful in determining the extent of the Martian MPB along the trajectory in association with the magnetic field data. In some of the examples the MPB appears to be preceded by a region where $|B|$ increases monotonically. At first sight this signature may be seen as associated to the boundary. However, both the variability in the orientation of the field and the level and variability of the superthermal electron fluxes measured by MGS MAG/ER clearly indicate that those regions are located within magnetosheath and therefore are not related to the MPB. MGS ER measurements also confirm that no multiple crossings of the MPB have been identified. Similar conclusions can be suggested for the Venusian MPB based on the variability of the magnetic field.

[27] It is interesting to compare the magnetic structure of the MPB with the properties of MHD directional discontinuities (DDs). *Lepping and Behannon* [1980] empirically estimated a threshold value on the relative normal component value for tangential discontinuities (TDs) that can be

Table 2. Main Parameters of the MVA for Different Venusian MPB Crossings by PVO

Orbit	SZA, deg.	Altitude, km	λ_2/λ_3	N	B_n, nT	θ_{Bn}, deg.	$\lvert B_n\rvert/\lvert B_0\rvert$
152	50	735	5.1	57	−15.7 ± 3.5	106.1 ± 4.2	0.28
170 (ib)[a]	56	619	15.0	53	−13.2 ± 1.8	101.8 ± 2.0	0.21
170 (ob)[a]	23	567	5.2	70	−9.3 ± 5.6	96.1 ± 3.8	0.11
180	11	480	10.1	174	−26.8 ± 2.6	103.4 ± 1.5	0.23
185	17	617	12.0	114	−14.9 ± 1.2	108.4 ± 1.7	0.32
635	8	495	9.2	173	−9.0 ± 0.8	99.4 ± 1.6	0.16

[a]Inbound (ib) and outbound (ob).

used to distinguish them from rotational discontinuities (RDs) using single-spacecraft magnetic field data. They found that all DDs where $|B_n|/|B_0| > 0.30$ are RDs with a 95% certainty, assuming that the fluctuations in the field are isotropic. According to this criterion the Martian and Venusian MPB crossings would resemble a TD rather than an RD. According to a recent study by *Knetter et al.* [2004], nonisotropic fluctuations can be important and bias MVA results. Consequently, they suggest that $\lambda_2/\lambda_3 > 10$ in order to have reliable results. The results presented in this study seem to reasonably match these criteria. At Mars the reliability of the results is supported by the agreement between the normal vectors deduced from MVA and from the MPB fit.

[28] In a study of the magnetic structure of Comet P/Halley MPB from Giotto spacecraft, *Neubauer* [1987] found similar properties: $(\lambda_2/\lambda_3)_{\text{inbound}} = 12.5$; $(\lambda_2/\lambda_3)_{\text{outbound}} = 19.4$ with $|B_n|/|B_0| = 0.05$ and 0.18, respectively, suggesting that it could be either a tangential discontinuity or a slowly propagating rotational discontinuity separating two regimes with strongly different plasma anisotropies, but only the latter type allows plasma and magnetic field transport as it occurs across the MPB. *Mazelle et al.* [1989] studied the expected changes in the plasma behavior across this boundary. As pressure balance must be satisfied for both types of discontinuity, in the case of a typical MHD tangential discontinuity we have

$$p_\perp + B^2/2\mu_0 = \text{constant}, \tag{3}$$

where $p_\perp$ is the total perpendicular plasma pressure. In the case of a rotational discontinuity, if **n** is the boundary normal and **P** is the total pressure tensor, pressure balance occurs when

$$\mathbf{n}\,\mathbf{P}\,\mathbf{n} + B^2/2\mu_0 = \text{constant}. \tag{4}$$

[29] This expression tends to equation (3) for a very slow RD. Magnetic field measurements at comets, Mars, and Venus show strong changes in the magnetic pressure (typically of a factor 4–10) at the MPB. Therefore strong changes in the plasma pressure are expected to be observed at the MPB.

[30] On the other hand, spacecraft observations and recent simulations show that the MPB is a boundary whose nature is based on the momentum transfer, via electromagnetic fields, from the solar wind to the planetary ion population [*Nagy et al.*, 2004]. For this reason the continuity relations for the magnetic field across the boundary may actually be far more complex than for MHD directional discontinuities. Interestingly, the values of the current density inferred from MGS MAG observations are consistent with the values predicted by three-dimensional two-ion two-fluid simulations at the MPB location.

[31] According to *Saunders and Russell* [1986], the magnetic tail boundary at Venus resembles a rotational discontinuity. These results are fully compatible with the idea that the MPB and the tail boundary are in fact connected [*Bertucci et al.*, 2003b] and that this boundary bounds the magnetic barrier region and the tail lobes [*Russell and Vaisberg*, 1983]. A similar study on the magnetic tail boundary of comet Giacobini-Zinner [*Slavin et al.*, 1986] from ICE magnetic field data led to a very good determination of the minimum variance direction: $(\lambda_2/\lambda_3)_{\text{inbound}} = 13.5$; $(\lambda_2/\lambda_3)_{\text{outbound}} = 8.1$. The results are consistent with the magnetic properties of tangential discontinuities and, according to the authors, the signatures suggest the presence of nonlinear processes (such as mass loading of heavy ions) that dramatically slow the interplanetary magnetic field lines to form the MPB.

[32] Analogue results were obtained by *Ness et al.* [1982] across what was identified as the magnetic tail boundary of Titan. The application of minimum variance analysis on Voyager 1 magnetic field data gives well-defined normal vectors for the inbound and outbound crossings $(\lambda_2/\lambda_3)_{\text{inbound}} = 22$; $(\lambda_2/\lambda_3)_{\text{outbound}} = 9$, with $|B_n|/|B_0| = 0.18$ and 0.21, respectively. This current sheet is associated to a strong enhancement of the draping magnetic field lines from Saturn's magnetosphere and is crossed almost at the same time as a cooling in the electron distribution is observed [*Hartle et al.*, 1982]. The presence of these concurrent features suggests that a MPB could be expected at Titan, at least when the angle between the direction of the incoming EUV flux from the Sun and either the corotational or magnetosheath flow is $<90°$ [*Wolf and Neubauer*, 1982].

[33] The determination of the thickness of the MPB is another important issue. On the other hand, the apparent thicknesses of the Martian and Venusian current sheets associated to the MPB seem to be of the order of the ion inertial length and smaller than the typical solar wind proton gyroradius [*Moses et al.*, 1988].

[34] Although a more accurate determination of the thickness of the MPB would imply a multispacecraft study, the distance traveled by the spacecraft along the normal direction gives a good approximation to the apparent thickness once the boundary is assumed at rest. *Dunlop et al.* [2002], using four-point Cluster observations, revealed that the Earth magnetopause undergoes accelerations up to 10 km s^{-2}, suggesting that apparent variations on boundary thickness could be partly due to variations in speed. For the Martian MPB crossing during orbit P342 the angle between the two vectors nears 60°, and the spacecraft remains in the boundary for ~2.5 min. Therefore it could be possible that the MPB had moved significantly during that lapse, leading to aliasing if magnetopause-type accelerations occur.

[35] Future work will be focused on a statistical study on the location of the Venusian MPB on the dayside in order to deduce its mean position by fitting a conic section. This will allow a comparison between the normal to the fit and the normal obtained from MVA. On the other hand, the measurements by the Automatic Space Plasma Experiment with Rotating Analyzer (ASPERA) investigation onboard Mars Express will supply new information on the ion inventory near the Martian MPB in order to understand the pressure variation across this boundary. Finally, Cassini magnetometer measurements around Titan will provide a more detailed characterization of the magnetic tail boundary and its counterpart on the hemisphere where the plasma flow points toward the satellite. These observations will undoubtedly expand our knowledge of the plasma boundaries generated from the interaction of a magnetized plasma wind with an unmagnetized atmospheric body.

[36] **Acknowledgment.** Arthur Richmond thanks Erika Harnett and Fritz M. Neubauer for their assistance in evaluating this paper.

References

Acuña, M. H., et al. (1992), The Mars Observer magnetic fields investigation, *J. Geophys. Res.*, *97*(E5), 7799–7814.

Acuña, M. H., et al. (1998), Magnetic field and plasma observations at Mars: Initial results of the Mars Global Surveyor Mission, *Science*, *279*, 1676–1680.

Bertucci, C., et al. (2003a), Magnetic field draping enhancement at the Martian magnetic pileup boundary from Mars Global Surveyor observations, *Geophys. Res. Lett.*, *30*(2), 1099, doi:10.1029/2002GL015713.

Bertucci, C., C. Mazelle, J. A. Slavin, C. T. Russell, and M. H. Acuña (2003b), Magnetic field draping enhancement at Venus: Evidence for a magnetic pileup boundary, *Geophys. Res. Lett.*, *30*(17), 1876, doi:10.1029/2003GL017271.

Brecht, S. (1997), Hybrid simulations of the magnetic topology of Mars, *J. Geophys. Res.*, *102*(A3), 4743–4750.

Breus, T. K., E. M. Dubinin, A. M. Krymskii, R. Lundin, and J. G. Luhmann (1991), The solar wind interaction with Mars: Consideration of Phobos 2 mission observations of an ion composition boundary on the dayside, *J. Geophys. Res.*, *96*(A7), 11,165–11,174.

Connerney, J. E. P., M. H. Acuña, P. J. Wasilewski, G. Kletetschka, N. F. Ness, H. Rème, R. P. Lin, and D. L. Mitchell (2001), The global magnetic field of Mars and implications for crustal evolution, *Geophys. Res. Lett.*, *28*(21), 4015–4018.

Crider, D. H., et al. (2002), Observations of the latitude dependence of the location of the martian magnetic pileup boundary, *Geophys. Res. Lett.*, *29*(8), 1170, doi:10.1029/2001GL013860.

Dunlop, M. W., A. Balogh, and K.-H. Glassmeier (2002), Four-point Cluster application of magnetic field analysis tools: The discontinuity analyzer, *J. Geophys. Res.*, *107*(A11), 1385, doi:10.1029/2001JA005089.

Grard, R., A. Pedersen, S. Klimov, S. Savin, A. Skalsky, J. G. Trotignon, and C. Kennel (1989), First measurements of plasma waves near Mars, *Nature*, *341*, 607–609.

Harnett, E. M., and R. M. Winglee (2003a), The influence of a mini-magnetopause on the magnetic pileup boundary at Mars, *Geophys. Res. Lett.*, *30*(20), 2074, doi:10.1029/2003GL017852.

Harnett, E. M., and R. M. Winglee (2003b), Asymmetries in the Martian magnetotail plasma as seen in 3D fluid simulations, *Eos Trans. AGU*, *84*(46), Fall Meet. Suppl., Abstract SM31C-1123.

Hartle, R. E., E. C. Sittler Jr., K. W. Ogilvie, J. D. Scudder, A. J. Lazarus, and S. K. Atreya (1982), Titan's ion exosphere observed from Voyager 1, *J. Geophys. Res.*, *87*(A3), 1383–1394.

Knetter, T., F. M. Neubauer, T. Horbury, and A. Balogh (2004), Four-point discontinuity observations using Cluster magnetic field data: A statistical survey, *J. Geophys. Res.*, *109*, A06102, doi:10.1029/2003JA010099.

Lepping, R. P., and K. W. Behannon (1980), Magnetic field directional discontinuities: 1. minimum variance errors, *J. Geophys. Res.*, *85*(A9), 4695–4703.

Lundin, R., A. Zakharov, R. Pellinen, H. Borg, B. Hultqvist, N. Pissarenko, E. M. Dubinin, S. W. Barabasj, I. Liede, and H. Koskinen (1990), Plasma composition measurements of the Martian magnetosphere morphology, *Geophys. Res. Lett.*, *17*(6), 877–880.

Mazelle, C., et al. (1989), Analysis of suprathermal electron properties at the magnetic pile-up boundary of comet P/Halley, *Geophys. Res. Lett.*, *16*(9), 1035–1038.

Mitchell, D. L., R. P. Lin, C. Mazelle, H. Rème, P. A. Cloutier, J. E. P. Connerney, M. H. Acuña, and N. F. Ness (2001), Probing Mars' crustal magnetic field and ionosphere with the MGS Electron Reflectometer, *J. Geophys. Res.*, *106*(E10), 23,419–23,427.

Moses, S. L., F. V. Coroniti, and F. L. Scarf (1988), Expectations for the microphysics of the Mars-Solar Wind interaction, *Geophys. Res. Lett.*, *15*(5), 429–432.

Nagy, A. F., et al. (2004), The plasma environment of Mars, *Space Sci. Rev.*, *111*(1–2), 33–114.

Ness, N. F., M. H. Acuña, K. W. Behannon, and F. M. Neubauer (1982), The induced magnetosphere of Titan, *J. Geophys. Res.*, *87*(A3), 1369–1381.

Neubauer, F. M. (1987), Giotto magnetic-field results on the boundaries of the pile-up region and the magnetic cavity, *Astron. Astrophys.*, *187*, 73–79.

Russell, C. T. (1978a), The magnetic field of Mars: Mars 3 evidence re-examined, *Geophys. Res. Lett.*, *5*(1), 81–84.

Russell, C. T. (1978b), The magnetic field of Mars: Mars 5 evidence re-examined, *Geophys. Res. Lett.*, *5*(1), 85–88.

Russell, C. T., and O. Vaisberg (1983), The interaction of the Solar Wind with Venus, in *Venus*, edited by D. M. Hunten et al., pp. 873–940, Univ. of Ariz. Press, Tucson.

Sauer, K., T. Roasch, U. Motschmann, K. Schwingenschuh, R. Lundin, H. Rosenbauer, and S. Livi (1992), Observations of plasma boundaries and phenomena around Mars with Phobos 2, *J. Geophys. Res.*, *97*(A5), 6227–6233.

Saunders, M. A., and C. T. Russell (1986), Average dimension and magnetic structure of the distant Venus magnetotail, *J. Geophys. Res.*, *91*(A5), 5589–5604.

Slavin, J. A., and R. E. Holzer (1982), The Solar Wind interaction with Mars revisited, *J. Geophys. Res.*, *87*(B12), 10,285–10,296.

Slavin, J. A., E. J. Smith, B. T. Tsurutani, G. L. Siscoe, D. E. Jones, and D. A. Mendis (1986), Giacobini-Zinner magnetotail: ICE magnetic field observations, *Geophys. Res. Lett.*, *13*(3), 283–286.

Sonnerup, B. U. Ö., and L. J. Cahill Jr. (1967), Magnetopause structure and attitude from Explorer 12 observations, *J. Geophys. Res.*, *72*(1), 171–183.

Sonnerup, B. U. Ö., and M. Scheible (1998), Minimum and maximum variance analysis, in *Analysis Methods for Multi-Spacecraft Data*, edited by G. Paschmann and P. W. Daly, *ISSI Sci. Rep. SR-001*, Eur. Space Agency, Paris.

Trotignon, J.-G., E. Dubinin, R. Grard, S. Barabash, and R. Lundin (1996), Martian planetopause as seen by the plasma wave system onboard Phobos 2, *J. Geophys. Res.*, *101*(A11), 24,965–24,977.

Vaisberg, O. (1992), The Solar Wind interaction with Mars: A review of results from early Soviet missions to Mars, in *Venus and Mars: Atmospheres, Ionospheres and Solar Wind Interactions*, *Geophys. Monogr. Ser.*, vol. 66, edited by J. G. Luhmann, M. Tatrallyay, and R. O. Pepin, pp. 311–326, AGU, Washington, D. C.

Vignes, D., C. Mazelle, H. Rème, M. H. Acuña, J. E. P. Connerney, R. P. Lin, D. L. Mitchell, P. Cloutier, D. H. Crider, and N. F. Ness (2000), The Solar Wind interaction with Mars: Locations and shapes of the bow shock and the magnetic pile-up boundary from the observations of the MAG/ER experiment onboard Mars Global Surveyor, *Geophys. Res. Lett.*, *27*(1), 49–52.

Wolf, D. A., and F. M. Neubauer (1982), Titan's highly variable plasma environment, *J. Geophys. Res.*, *87*(A2), 881–885.

Zakharov, A. V. (1992), The plasma environment of Mars: Phobos Mission results, in *Venus and Mars: Atmospheres, Ionospheres and Solar Wind Interactions*, *Geophys. Monogr. Ser.*, vol. 66, edited by J. G. Luhmann, M. Tatrallyay, and R. O. Pepin, pp. 327–344, AGU, Washington, D. C.

Zhang, T. L., J. G. Luhmann, and C. T. Russell (1991), The magnetic barrier at Venus, *J. Geophys. Res.*, *96*(A7), 11,145–11,153.

M. H. Acuña and J. A. Slavin, NASA Goddard Space Flight Center, Mail Code 696, Greenbelt, MD 20771, USA.

C. Bertucci, Blackett Laboratory, Space and Atmospheric Physics, Imperial College London, Prince Consort Road, London SW7 2BZ, UK. (c.bertucci@imperial.ac.uk)

C. Mazelle, Centre d'Etude Spatiale des Rayonnements, CNRS/UPS, 9, Avenue du colonel Roche, BP 4346, 31028 Toulouse Cedex 4, F-31028 France.

C. T. Russell, Institute of Geophysics and Planetary Physics, University of California, 3845 Slichter Hall, 405 Hilgard Avenue, Los Angeles, CA 90095-1567, USA.

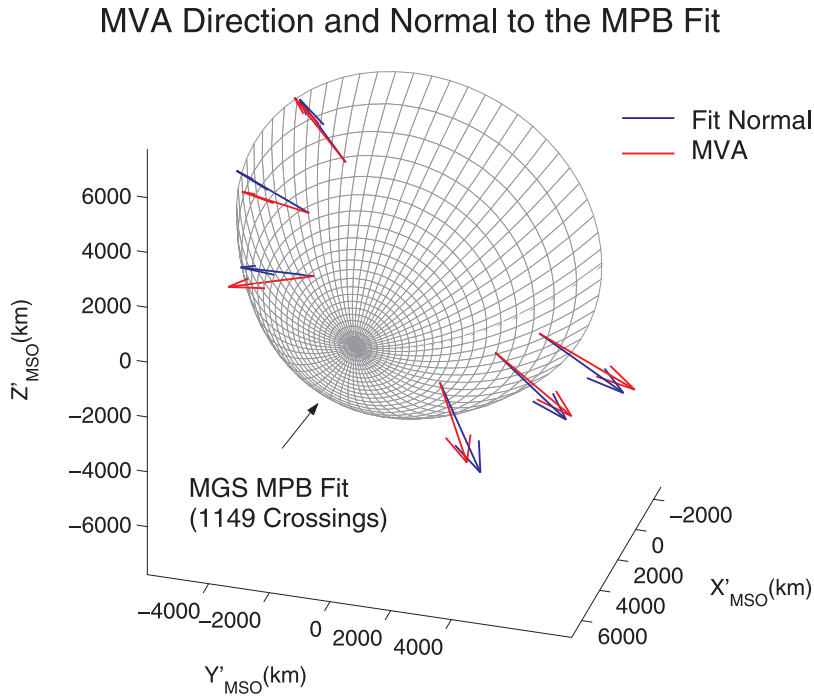

Figure 3. Comparison between minimum variance direction and the normal expected from a MPB ellipsoid fit from 1149 Martian MGS crossings based on *Vignes et al.* [2000] work (blue arrows). Sketch is represented in 4°-aberrated MSO coordinates.